



Flow and heat transfer during compression resin transfer moulding of highly reactive epoxies

A. Keller^a, C. Dransfeld^a, K. Masania^{b,*}

^a Institute of Polymer Engineering, FHNW University of Applied Sciences and Arts Northwestern Switzerland, Klosterzelgstrasse 2, 5210, Windisch, Switzerland

^b Complex Materials Group, Department of Materials, ETH Zürich, 8093, Zurich, Switzerland

ARTICLE INFO

Keywords:

Compression RTM
Highly reactive epoxies
Flow simulation

ABSTRACT

Fast-cure epoxy systems are used for the mass production of composite parts with cycle times in the minute range. One of the major difficulties observed when processing fast-cure resins is their strong exothermic reaction during cure. This may result in a significant temperature overshoot and large temperature gradients over the thickness, and therefore gradients, in glass transition temperature, shrinkage and residual stress. Hence, the cure reaction during the injection, impregnation, compaction and curing stages need to be understood and optimised in order to reduce cycle time without sacrificing mould filling and part quality. A possibility to process such highly reactive epoxies is the compression resin transfer moulding process (CRTM), where the preform is impregnated in through-thickness direction, leading to reduced cycle times. The aim of this work is to identify processing constraints that the different CRTM variations present when using fast-curing resins. We have developed a multi-physics model to compare three variations of the CRTM process: gap injection, direct dosing and wet pressing, by studying their fluid flow and the exothermic reaction. The models show the importance of the injection strategy to avoid temperature overshoot, which can occur before the part is fully impregnated. Our results show that when impregnation time is a limiting factor, wet pressing appears to be a favourable approach for fast composite processing, doubling the available impregnation time before gel.

1. Introduction

Mass production of carbon fibre reinforced polymers (CFRP) may be achieved by using liquid composite moulding processes, as they enable a higher degree of automation compared to standard manufacturing processes. However, parameters such as injection strategy or cure temperature must be carefully chosen in order to minimise cycle time and costs without sacrificing the final part quality, which starts with the appropriate choice of the process itself [1]. Baskaran et al. [2] studied the cost of an automotive roof with 100,000 parts per year manufactured with standard resin transfer moulding (RTM), high pressure RTM (HP-RTM) and compression resin transfer moulding (CRTM). Costs were clearly reduced using manufacturing approaches that decrease cycle time such as CRTM, which explains the increasing interest in this manufacturing approach. In this process, the mould is opened to provide a gap for resin injection on top of the preform. The following compression stage is dominated by through thickness impregnation of the preform, which significantly reduces flow paths, impregnation times and thus processing costs [2,3].

Through thickness impregnation during CRTM reduces the flow

length, L , and hence the impregnation time by a factor of L^2 compared to in-plane impregnation, where L represents the length of a part.

This dramatic reduction in impregnation time allows the use of very fast-curing resins. However, the use of fast-cure resins leads to new challenges in handling and processing of the material due to the high exothermic reaction associated with the very fast reactions [4,5]. This can cause large temperature overshoots and gradients in temperature which can lead to variations in the degree of cure and viscosity inside the part, internal stresses or even material decomposition [4,6]. Hence, the cure reaction during the injection, impregnation, compaction and curing stage needs to be understood and optimised in order to reduce cycle time without compromising mould filling and therefore part quality.

Numerical simulations for mould filling are increasingly used to design tooling and place gate positions [7–9], as well as to gain understanding of the CRTM impregnation process [10–13]. The CRTM process has some variations, which differ slightly in their procedure, but strongly influence the impregnation process due to their differing initial boundary conditions. These differences become even more relevant when using fast-curing resins because exothermic heat

* Corresponding author.

E-mail address: kunal.masania@mat.ethz.ch (K. Masania).

<https://doi.org/10.1016/j.compositesb.2018.07.041>

Received 4 May 2018; Received in revised form 12 July 2018; Accepted 22 July 2018

Available online 23 July 2018

1359-8368/ © 2018 Elsevier Ltd. All rights reserved.

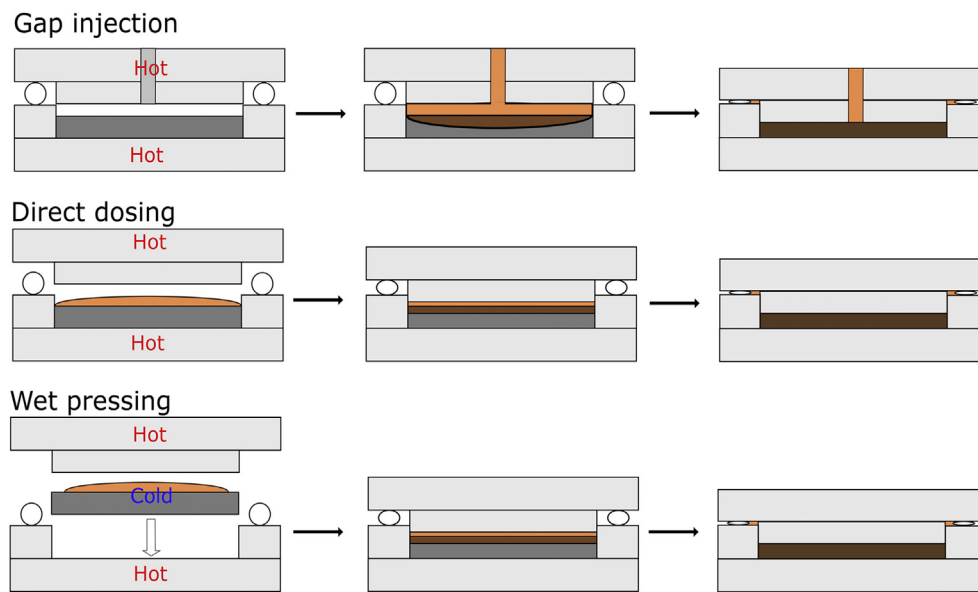


Fig. 1. Variations of the compression resin transfer moulding (CRTM) processes shown schematically.

generation is more dramatic, and the shorter process times reduce time governed homogenisation of heat flow and temperature.

This work considers three cases: gap injection, direct dosing and wet compression as possible CRTM procedures as shown in Fig. 1 and described in Table 1. The first two cases utilise a preheated tool and preform with different injection strategies, namely injection into a cavity (gap injection), or dispensing resin onto the preheated preform in the tool (direct dosing). In the third, the wet pressing process, the resin and preform are combined outside of the tooling and simultaneously placed in the preheated mould.

In all three processes, the resin heats up further during the compression stage from direct contact with the mould cavity, reducing viscosity and simultaneously saturating the fibres. Compaction pressure also increases the fibre volume content as the fibres move closer to their final thickness. Lastly, the tool is closed and most of the tool pressure is transmitted through the hydrostatic pressure in the resin with some stress on the fabric preform.

Due to their initial differences, temperature equilibrium between the preform, resin and preheated mould varies for these three processes, which can have a significant effect on the final part's thermo-mechanical properties such as reduced strength, faster initiation of cracks and delamination. The aim of this work is therefore to determine processing constraints from the different CRTM methods when using fast-curing epoxy resins.

We have developed a multi-physics model to compare different methods for the injection strategy for CRTM by fluid flow and the exothermic reaction using Comsol Multiphysics, which has been used for fluid flow [14–16] and heat transfer [16,17] in composites. The models are solved in a two-dimensional section where main focus is set on temperature progression and possible injection times before gelation and model validation with experimental measurements.

Table 1
Variations of the compression resin transfer moulding (CRTM) processes.

CRTM-Method	Initial conditions	Resin dosing	Impregnation	Curing
Gap injection	Preheated mould and preform	Injected into preheated mould	Applied pressure engages impregnation and compaction of preform	Cured under pressure
Direct dosing	Preheated mould and preform	Dosed onto preheated preform		
Wet pressing	Preheated mould, cold preform	Dosed onto cold preform		

2. Materials and experimental methods

A diglycidyl ether of bisphenol A (DGEBA) epoxy resin with an epoxy equivalent weight (EEW) of 181.5 g eq^{-1} , XB 3585 from Huntsman Advanced Materials, Switzerland, was used. The curing agent was a mixture of diethylenetriamine and 4,4'-isopropylidenediphenol, XB 3458 from Huntsman Advanced Materials, Switzerland, which was combined with the DGEBA at a stoichiometric ratio of 100:19 by weight of epoxy to hardener. A unidirectional plain weave carbon fibre fabric from Suter Kunststoffe AG with 3 K tows and an areal weight of 140 g/m^2 was used. The weft yarn was an E-glass fibre with 1 K tows and made up 12% of the preform volume. The laminate was composed of 20 plies to form a 3.85 mm thick unidirectional laminate.

Of the three processes described in Table 1, direct dosing was validated experimentally. A compression mould with vertical shut-off with cavity dimension 380 mm by 180 mm was used. The mould was isothermally heated with circulating oil to a temperature of $90 \text{ }^\circ\text{C}$ and moulding trials were carried out in a 200 kN hydraulic press (Lauffer, Germany), where a maximum pressure of 20 bar was applied. Temperature sensors were placed inside the preform and on top into the resin to perform the in situ measurements.

Isothermal measurements were conducted using a Mettler DSC 1 with 5 mg of resin. The pre-heated furnace was manually opened and the sample placed into the cell.

3. Governing equations and material characterisation

To account for heat transfer phenomena, fibre compaction and rheokinetics in the multiphysics model in section 4, the following governing equations and material models have been used.

3.1. Flow through a porous media

Viscous flow through a porous media is commonly modelled using Darcy's law. Combined with mass conservation and a source term to account for the preform compaction; Darcy's law results in Refs. [10,18].

$$\nabla \cdot \left(-\frac{K}{\eta} \nabla p \right) = -\frac{1}{V_f} \frac{\partial V_f}{\partial t} \quad (1)$$

where K is the permeability, η the viscosity, p the pressure and V_f the fibre volume content.

Terzaghi's law [19] can be used to model the pressure distribution between resin and preform.

$$p_{ap} = \sigma_{pref} + p \quad (2)$$

where p_{ap} is the applied pressure from the top stamp, σ_{pref} the preform stress and p the fluid pressure.

A level set method was used to track the flow front in the following form, as implemented in Comsol Multiphysics 5.0 [20]:

$$\frac{\partial \phi}{\partial t} + \mathbf{u} \cdot \nabla \phi = \gamma \nabla \cdot \left(\varepsilon_{is} \nabla \phi - \phi(1 - \phi) \frac{\nabla \phi}{|\nabla \phi|} \right) \quad (3)$$

where γ is the re-initialisation parameter in (m/s) which is used to compute the steady state solution after each time step to avoid numerical smearing, ε_{is} is a parameter controlling the interface thickness and which typically depends on the mesh size [21], \mathbf{u} is the velocity and ϕ is the level set function, which is zero for non-saturated areas and one in the saturated areas.

The convective term of the level set may carry on numerical effects. A smoothing function was introduced to prevent accumulation of numerical noise

$$\phi_{smooth} = \frac{1}{1 + \exp(\delta(-\phi + 0.5))} \quad (4)$$

where δ defines the width of the transition region.

The separation of phases requires material properties to be defined for the air and the resin phase as

$$f = f_{air} + (f_{air} - f_{composite}) \phi_{smooth} \quad (5)$$

where f denotes a material parameter such as density, ρ , viscosity, η , thermal conductivity, k , or specific heat capacity, C_p , with the parameters used for modelling given in Table 2.

3.2. Heat transfer

During cure, the resin temperature is a result of both an external heat source (tool, preform) and the internal heat generation during the curing reaction. The internal heat generation mainly depends on the cure kinetics of the epoxy, which can be described with Eq. (6).

$$\rho_c C_p \frac{\partial T}{\partial t} + \rho_r C_{pr} \mathbf{v} \cdot \nabla T + \nabla \cdot (-k \nabla T) = \rho_r H_{tot} \frac{d\alpha}{dt} (1 - V_f) \quad (6)$$

where T is the temperature, ρ_r and ρ_c are the densities of the resin and the composite respectively, C_p the heat capacity, \mathbf{v} the volume averaged

Darcy velocity, k the thermal conductivity tensor, H_{tot} the total heat of reaction, $d\alpha/dt$ the reaction rate and V_f the fibre volume fraction.

The thermal conductivity, k , for a unidirectional composite in transverse direction is given by the rule of mixtures

$$k_2 = k_3 = \frac{1}{\frac{1}{k_f} V_f + \frac{1}{k_m} (1 - V_f)} \quad (7)$$

where the subscripts f and m denote fibre and matrix respectively.

The density and heat capacity are similarly given in the following form

$$f = f_f V_f + f_m (1 - V_f) \quad (8)$$

where f denotes a material parameter.

3.3. Rheo-kinetics

The reaction rate of the studied epoxy was previously modelled [4] based on the approach of Ruiz et al. [22] in the following form:

$$\frac{d\alpha}{dt} = k_1 e^{\left(-\frac{E_1}{T} \left(\frac{T_{ref}}{T} - 1 \right) \right)} \sum_{i=0}^m G_i \alpha^i (\alpha_{max}(T) - \alpha)^n \quad (9)$$

$$\text{with } G(\alpha) = \frac{G_1 \alpha^4 + G_2 \alpha^3 + G_3 \alpha^2 + G_4 \alpha + G_5}{G_6 \alpha^2 + G_7 \alpha} \quad (10)$$

$$\text{and } \alpha_{max} = \frac{T_c - T_{g0}}{(T_c - T_{g0})(1 - \lambda) + (T_{g\infty} - T_{g0})\lambda} \quad (11)$$

$$\text{and } n = n_s T_c + n_i \quad (12)$$

With the modelling parameters that were implemented, summarised, in Table 3.

The viscosity was modelled based on the approach of Geissberger et al. [23] in the following form:

$$\eta(t, T) = \sum_{t_i, \Delta t_i=1}^n A_1 \exp\left(\frac{E_1}{RT(t_i)}\right) \exp\left[A_2 \exp\left(\frac{E_2}{RT(t_i)}\right) \Delta t_i (A_4 T(t_i) + E_4)\right] \cdot \frac{1}{E_3} \left[\gamma_0 + A_3 \exp\left(A_2 \exp\left(\frac{E_2}{RT(t_i)}\right) \frac{\Delta t_i (A_4 T(t_i) + E_4)}{E_3}\right) \right] \quad (13)$$

A and E are fitting parameters, T is the temperature, t the time and R is the universal gas constant which are given in Table 4.

3.4. Moving mesh

A moving mesh based on the arbitrary Lagrangian-Eulerian (ALE) method was used to account for the change of thickness during compaction of the preform. Remeshing was automatically performed to ensure good mesh quality once the quality factor was lower than 0.2. Where the mesh quality is an indication of the length to width ratio of the elements.

Table 2

Material parameters used for the heat transfer model.

	Epoxy	Preform	Air [20]
Heat conductivity, k (W/(m K))	0.2	1.7	0.02897p/8.314/T
Specific heat capacity, C_p (J/(kg K))	1336 + 9.3 T (°C)	577 + 6.85 T (°C)-0.018T ² (°C) [28]	1047-0.37 T + 9.45E-4T ² -6.02E-7T ³ +1.29E-10T ⁴
Density, ρ (kg/m ³)	1150	1700	-0.00228 + 1.155E-4T-7.90E-8T ² +4.12E-11T ³ -7.44E-15T ⁴

Table 3
Fitting parameters for the cure kinetic model.

Name	Symbol	Value	Name	Symbol	Value
Polynomial parameter	G ₁	−1351	Reaction exponent factor slope	n _s	0.018
Polynomial parameter	G ₂	−2678	Reaction exponent factor intercept	n _i	−5.2367
Polynomial parameter	G ₃	10194	Frequency factor	k ₁ (s ^{−1})	0.00309
Polynomial parameter	G ₄	4338	Activation energy	E ₁	22.28
Polynomial parameter	G ₅	−5.208	Reference temperature	T _{ref} (K)	350
Polynomial parameter	G ₆	587	T _g of the uncured resin	T _{g0} (K)	246.15
Polynomial parameter	G ₇	4570	T _g of the cured resin	T _{g∞} (K)	394.4
			Parameter for α _{max} model	λ	0.32

Table 4
Parameters used for the rheological model.

Parameter	Unmodified epoxy
A ₁	1.32 × 10 ^{−9}
E ₁	52931
A ₂	7518
E ₂	−38710
A ₃	2.7
E ₃	2.2
A ₄	0.0029
E ₄	−0.236

3.5. Measuring preform compaction

Preform compaction was measured in a universal testing machine (Walter & Bai, Switzerland) between two parallel plates with a diameter of 136 mm and a constant velocity of 0.5 mm/min. Machine compliance was measured and subtracted from the machine-measured displacement. Measurements were conducted for both the dry and silicone oil impregnated wet preform, with a viscosity of 0.1 Pa. A preform of 30 unidirectional layers were measured to eliminate local effects of nesting and tow movement. The preform pressure as a function of the V_f was described using a power law in the following form:

Table 5
Modelling parameters of the compaction tests.

	A	B	R ²
Dry	2.23 × 10 ^{−9}	20.3	0.9993
Wet	6.25 × 10 ^{−7}	11.3	0.9993

$$\sigma(V_f) = A \cdot V_f^B \tag{14}$$

where A and B are the fitting parameters given in Table 5 with their corresponding coefficient of determination.

3.6. Measuring preform permeability

Preform samples with a diameter of 79 mm were cut with a Zünd G3 M-2500 cutter and then placed into the permeability jig. Silicone oil was injected from the bottom side with a pressure of 0.05 bar through a 10 mm-thick stack of samples until a constant flow could be measured. Measurements were then performed under saturated conditions for different flow rates. In case of zero preform compaction, i.e. with a V_f value of 0.39, the measurement was analysed with an injection pressure of 0.05 bar. For higher V_f values, i.e. 0.45, the pressure was constantly increased and a linear regression of the mass flow as a function of pressure was used to calculate the permeability.

The saturated permeability values in through thickness direction

were calculated according to Darcy's law and fitted using a second order polynomial term (Equation (15)).

$$K_z = 1.92 \times 10^{-11} V_f^2 - 2.72 \times 10^{-11} V_f + 9.66 \times 10^{-12} \tag{15}$$

4. Numerical model

4.1. Numerical domain

The problem was modelled in Comsol as a through thickness two-dimensional section with a width of 180 mm, with the numerical domain given in Fig. 2.

4.2. Modelling direct dosing and wet pressing

The following boundary conditions were used to model heat transfer and exothermic reaction of the resin on top of the preheated (direct dosing) or cold (wet pressing) preform, as shown in Fig. 2. A convective heat flux of 10 W/(m² K) was applied to the top boundary of the resin and a constant temperature was used at the bottom boundary, representing the mould. The thickness of the resin domain was suitably adjusted for volume conservation as a moving mesh that was a function of the flow velocity at the top boundary of the resin.

Impregnation can already begin during the heating process due to gravity, capillary forces and the relatively low viscosity at higher temperatures (as low as 0.1 Pas). The flow velocity is given as:

$$v = \frac{K}{\eta(1 - V_f)} (\nabla p + \rho g) \tag{16}$$

where K is the permeability, ρ the density, g the acceleration of gravity and η the viscosity.

The capillary pressure was calculated according to Bernet et al. [24].

$$P_c = \frac{2 \gamma \cos(\theta)}{d_f} \frac{V_f}{1 - V_f} \tag{17}$$

where γ is the resin surface tension, set to 0.035 N/m [25], θ is the contact angle (30° [26]), d_f is the fibre diameter and V_f the fibre volume content.

4.3. Modelling of compression-impregnation

The time between the first contact of the resin with the preform and start of controlled impregnation was experimentally determined to take about 45 s for direct dosing. Likewise, the initial conditions, i.e. temperature and viscosity were taken from the numerical model after 45 s for direct dosing (preheated preform). Since closing of the mould is typically velocity driven, a rate of 0.5 mm/s was used until the maximum pressure of 20 bar was reached. Effects of gravity and capillary pressure were not included in the compression-impregnation model because of the relatively high pressures. A pressure curve was used as a boundary condition on the top stamp to describe the pressure due to

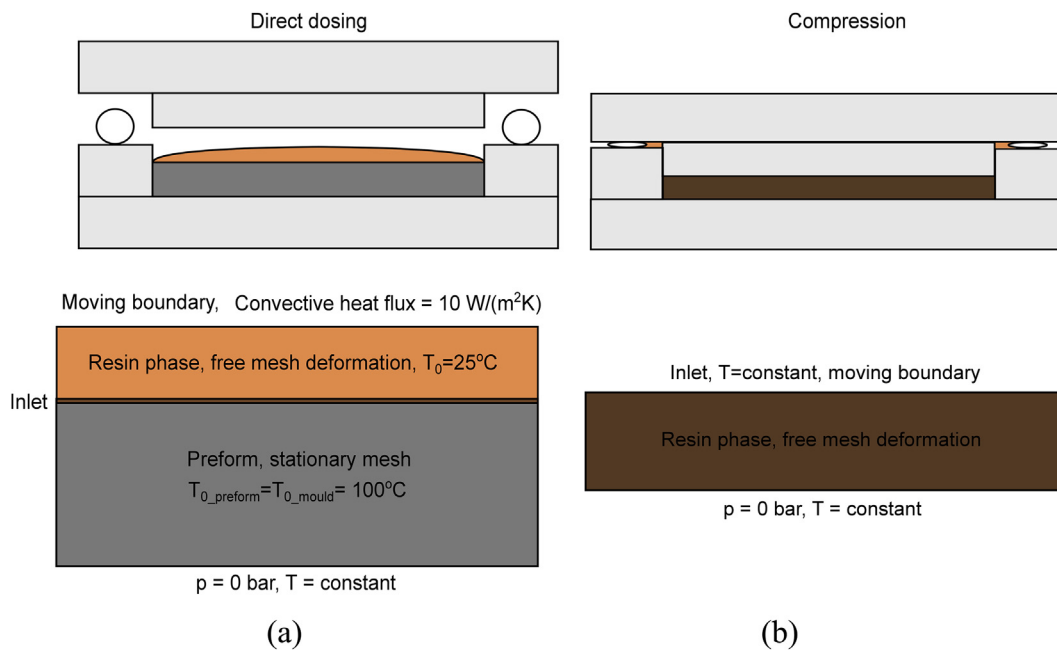


Fig. 2. Numerical domain of the models for (a) direct dosing and (b) compression with boundary and domain conditions.

constant velocity closing (0.5 mm/s) and a zero pressure boundary condition was applied to the bottom of the mould. A constant temperature of 100 °C was applied on the top and bottom boundary. In our experiments, we noticed that the thermal mass of the mould acted as a heat sink. Therefore, only little increase in the mould temperature due to exothermic heat from the resin was recorded. The peak temperature of the resin was not influenced by the large thermal mass of the mould because the exothermic reaction of the resin curing progressed rather quickly.

4.4. Modelling gap injection

The preform and mould were assumed to be preheated at 100 °C at the start of gap injection. A constant temperature boundary condition was used at the bottom, in accordance with the models for direct dosing and wet pressing. The upper part of the mould was included as a steel mould with an initial temperature of 100 °C.

4.5. Numerical solver

The models were solved in Comsol Multiphysics 5.0 using the “Multifrontal massively parallel sparse direct solver” (MUMPS). For the fully coupled nonlinear solver, we used the damped Newton method to obtain convergence by varying the damping factor until the solution converges [20]. A triangular free mesh was used and the element size was set to 0.68 mm after a mesh sensitivity study to ensure convergence of the models.

5. Results and discussion

5.1. Modelling and experimental validation of direct dosing and wet pressing without compaction

The following models aim to predict the possible impregnation times of direct dosing and wet pressing, and therefore do not include mould closing and preform compaction. The mould closing was taken into account in the models in the next section.

The temperature and degree of cure evolution with time during impregnation for the case of direct dosing onto the preheated preform is

shown in Fig. 3 (a). The models illustrate an initial temperature increase as a result of the heat transfer between the preform and resin. A rapid exothermic temperature increase was predicted at 73 s, indicated by the arrows in Fig. 3 (a). Interestingly, the internal heat generation due to the start of curing becomes so dominant that it exceeds the tool temperature at this point. Hence, including resin kinetics into the heat transfer model as a source term in eq. (6) clearly plays an important role in describing temperature dependent values such as viscosity, so must be included to accurately capture impregnation behaviour.

Isothermal differential scanning calorimetry (DSC) measurements at different temperatures were performed to quantify the exothermic heat during cure. The measurements show that a large amount of heat was released in the beginning of the reaction with the maximum heat flow measured at a degree of cure of 0.1 (Fig. 3 (b)). The maximum heat flow is very high in comparison to standard curing epoxies. For example RTM 6, an epoxy system which is commonly used in the aerospace industry for infusion processes has a 20 times lower maximum heat flow at 180 °C, compared to the studied, fast-cure epoxy at 100 °C despite having a similar total heat of reaction [27]. Hence, the temperature can progress rapidly during cure if the exothermic heat is not sufficiently accounted for in the process and mould design.

Fig. 4 (a) displays the modelled temperature progression at two different locations, in the resin phase as per Fig. 3 (a) and at the bottom of the preform. The resin that has impregnated the preform cures faster compared to the resin on top of the fibres, showing the need to incorporate gravity driven preform saturation for this process. Unlike when using gap injection with a partially closed mould, the resin is not in contact with the preheated steel but is exposed to air. The constant heat flux with air reduces the temperature of the distributed resin on top of the preform.

In order to verify these findings, experiments of the temperature progression shown in Fig. 4 (b) confirm these observations. Impregnation due to gravitational and capillary forces, as predicted by the model, takes place with decreasing viscosity and curing appears to start at the bottom where the resin is in contact with the preheated preform and mould.

The temperature progression inside the preform was replicated very well. Some deviation can be observed for the temperature measured on top of the preform. This is believed to be because of the thickness of the

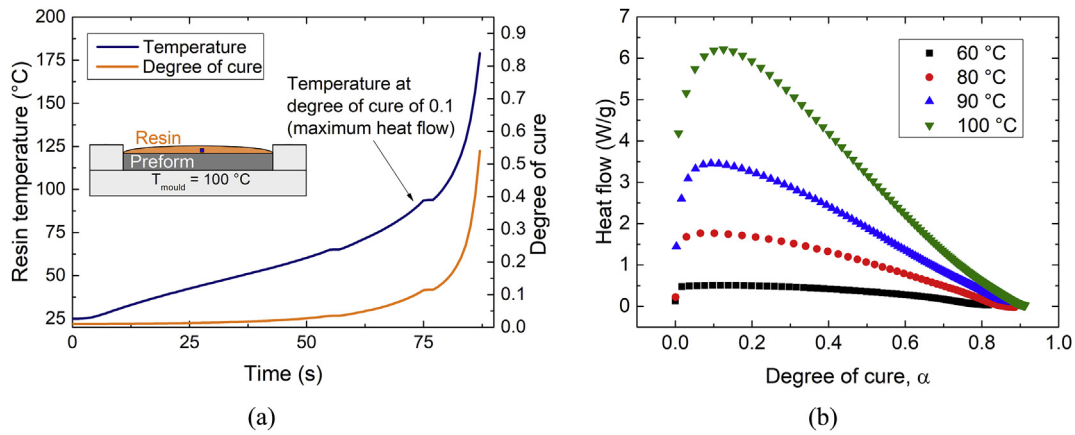


Fig. 3. Direct dosing: (a) Correlation between modelled temperature progression and degree of cure of the resin. (b) Heat flow for isothermal differential scanning calorimetry (DSC) measurements of the pure resin.

resin film on top of the preform. Although it was adapted via a moving mesh, error in the fit may be observed due to a slightly different flow behaviour in the experiments as a result of the dual-scale flow behaviour in the preform, which have not been included in this model.

Since the effect of exothermic heat control is so critical to the process, we modelled the temperature and cure progression for a wet pressing case, where a cold preform and resin are simultaneously added to a preheated tool. Our models show that the possible impregnation time increases by a factor of almost two when using the wet pressing approach compared to direct dosing, as shown in Fig. 5. The initial, strong exothermic reaction appears to be better controlled in the wet pressing. The viscosity rises more gradually for wet pressing, whereas a steep increase was modelled for direct dosing, which leads to gelation within only a few seconds. Since dosing or gap injection of the resin is not used for this process, further cycle time can be saved for less complex structural parts when adopting the wet pressing process.

5.2. Modelling of resin-dosing with compression-impregnation

The compression stage of CRTM was further modelled for the direct dosing process. Start of compression was taken 45 s after the start of direct dosing.

By studying the temperature data at different regions in the composite plate, the models show that the curing within the tool is non-uniform at 100 °C (Fig. 6). A maximum temperature of 121 °C was predicted in the middle of the 3.85 mm thick plate, having a global V_f of 0.6 as it can be seen in Fig. 6 (a) and (b). The increase of V_f (up to 0.6)

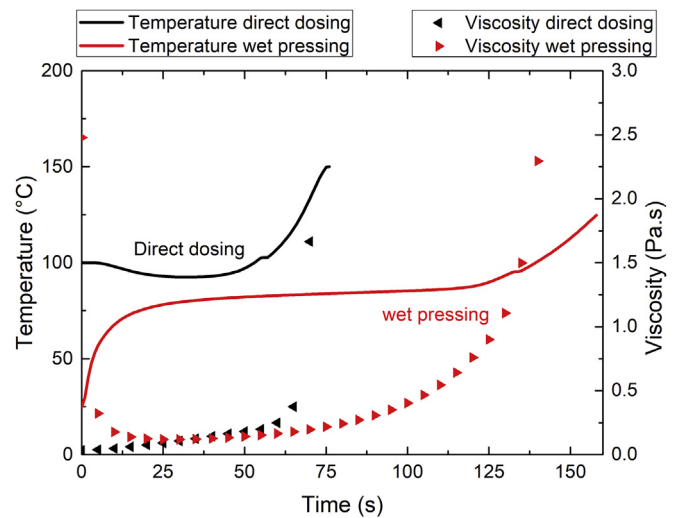


Fig. 5. Numerical results show temperature and viscosity progression for direct dosing (preheated preform) and wet pressing (cold preform) CRTM.

reduces the exothermic mass, and hence the resin temperature overshoot compared to the model of direct dosing before compaction.

A significant degree of cure gradient over the thickness was calculated and is shown in Fig. 6 (c) and (d), with a maximum variation of 0.12 with a mould temperature of 100 °C. A gelation time of 135 s was

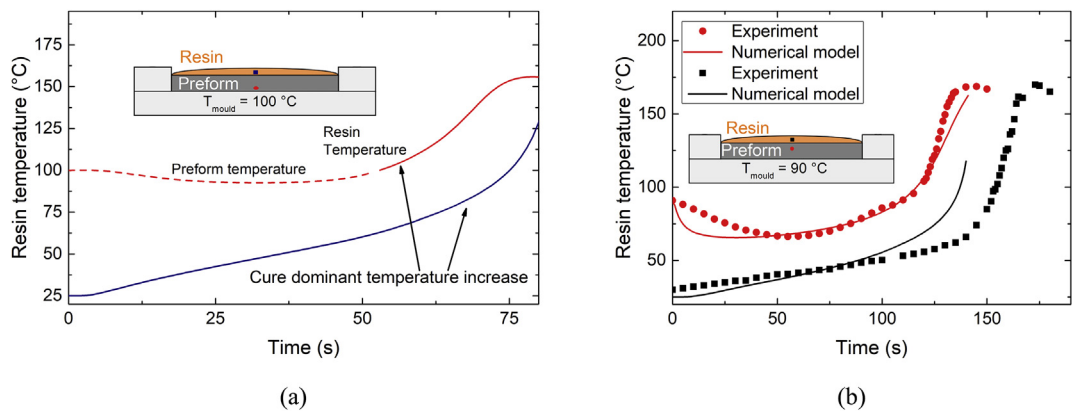


Fig. 4. Direct dosing: (a) The modelled resin temperature progression at two different locations with a mould temperature of 100 °C and (b) validation with experimentally measured values for a mould temperature of 90 °C using direct dosing.

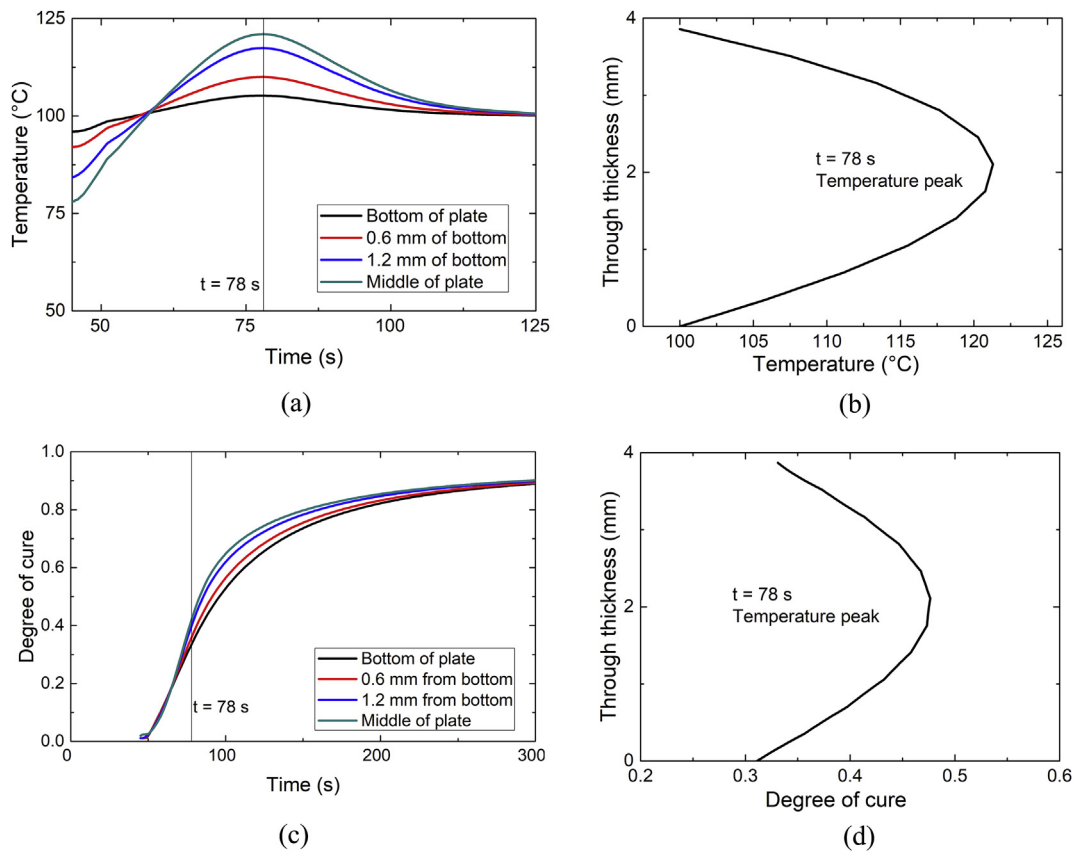


Fig. 6. Direct dosing compression stage: numerical results for (a) temperature versus time at different locations through the thickness of the composite plate, (b) temperature distribution over the thickness after 78 s (time of highest peak) (c) Degree of cure conversion at different locations through the plate thickness and (d) degree of cure distribution through the thickness after 78 s (time of highest peak) with the initial mould temperature set to 100 °C.

calculated for the edges and only 90 s at the location of the highest temperature overshoot in the middle of the plate. A more uniform degree of cure of 0.9 was calculated after 5 min, whereas the final degree of cure of 0.92 was predicted for 7 min. These values are in good agreement with differential scanning calorimetry (DSC) measurements using a heating rate of 10 K/min to obtain values for degree of cure of 0.88–0.93.

Even when adapting the process temperature to 90 °C in order to

manage resin temperature overshoot, a 9 °C increase in temperature was observed, shown in Fig. 7. A maximum variation of 0.08 in the degree of cure was calculated with a mould temperature of 90 °C.

5.3. Pressure distribution and impregnation

During impregnation, two different factors account for the maximum applied pressure. In the beginning, when the resin is on top of the

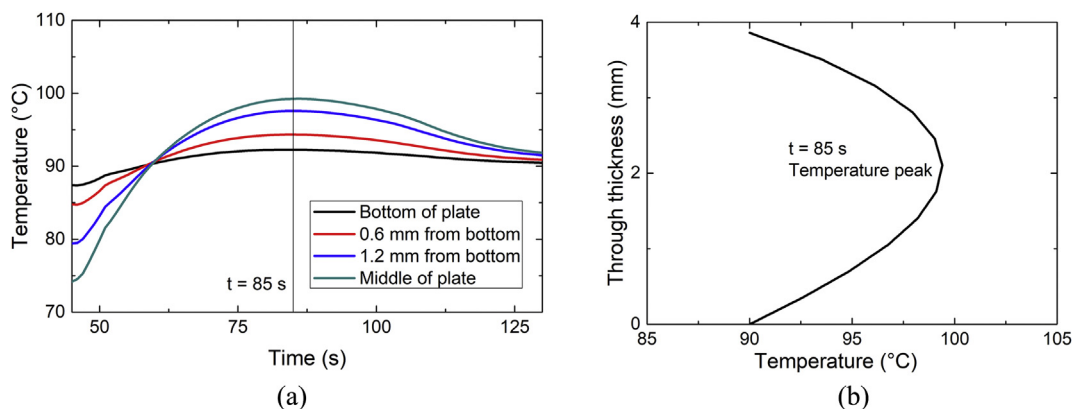


Fig. 7. Direct dosing compression stage (a) numerical temperature versus time at different locations through the thickness of the composite plate and (b) temperature distribution over the thickness after 84 s (time of highest peak) with the initial temperature at 90 °C.

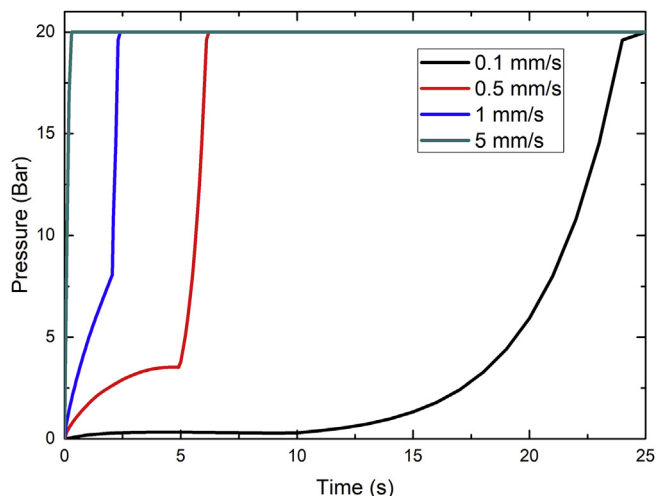


Fig. 8. Simulated pressure profile during impregnation and compaction.

preform, the pressure is given by the closing velocity and the interaction between preform and resin. Eventually the mould will be in contact with the preform, which will drastically increase the pressure, similar to the compaction tests until a predefined maximum pressure is reached and the mould closing velocity is zero. The resulting pressure from the simulation is shown in Fig. 8 with a closing velocity between 0.1 and 5 mm/s. One can notice the tremendous increase of pressure at higher velocities, which can decrease the preform permeability. A more gradual pressure increase can lead to a more uniform flow front and reduced air inside the fibre tows due to the dual-scale nature of the preform, however a slow closing speed might be compromised by the increase in viscosity of the resin.

5.4. Modelling gap injection

The effect of the injection pressure was studied for one case with a lateral flow length of 50 mm, a gap thickness of 2 mm and an uncompressed preform thickness of 6 mm. The metered resin flows in the gap between the preheated preform and mould because of the higher relative permeability before impregnating the preform. Heat transfer between the steel mould and the resin leads to a rapid temperature increase, which accelerates the cure reaction and generates exothermic heat in the resin, which further increases the temperature. With small injection pressures, and hence slow resin movement, the temperature in the resin increases while the resin is still in the gap between the mould and the preform.

When the injection pressure is sufficiently high, the gap is filled within seconds and the resin starts to impregnate the preform. This reduces the amount of pure resin, and hence reduces the exothermic reaction. During injection into the gap, a small amount of resin already impregnated the preform.

To demonstrate this effect, Fig. 9 shows temperature time profiles for the maximum resin temperature when using different injection pressures. At a pressure of 0.5 bar, temperature overshoots of 80 °C up to temperatures of 180 °C were predicted. When the pressure was increased, and hence impregnation time reduced, the temperature overshoot reduced to 50 °C at 1 bar and to 40 °C at 2 bar injection pressure. This implies that resin stagnation can lead to very high temperatures in the tool. During injection, the maximum temperature gradually decreases. Typically, the maximum temperature is observed locally at the flow front in the gap, which partially impregnates the preform and therefore gradually decreases the local resin temperature. This effect can be seen at pressures of 1 and 2 bar, where more through-thickness impregnation takes place during gap injection.

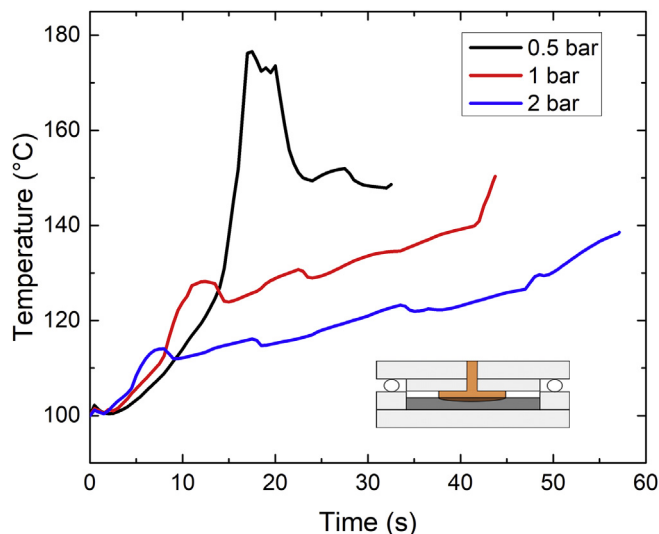


Fig. 9. Numerical results showing the maximum temperature within the resin domain during gap injection (before the compression phase) depending on the pressure, where the initial temperature of the resin and mould are 100 °C initially.

6. Conclusions

The strong exothermic reaction and resulting temperature overshoot observed with fast-curing resins can prevent full impregnation of a composite parts, lead to internal stresses or even material decomposition. In this study fluid flow and the exothermic reaction of three CRTM processes: gap injection, direct dosing and wet pressing were studied. The main focus was set on the injection stage of all processes, as the use of fast-curing resins leads to further complications during filling, i.e. significant viscosity changes and strong exothermic reaction. The models were experimentally validated for the direct dosing CRTM process.

Preform saturation during resin injection or gravity driven flow for the direct dosing and wet pressing processes becomes a crucial parameter to be modelled, as it highly influences the heat transfer and resulting exothermic reaction. For example, the models and experiments showed that the resin cures faster at the bottom of the mould than on top of the fibres for the direct dosing process.

Gap injection, which is typically used for CRTM has the highest potential risk of gelation before the part is impregnated due to the contact of the resin with the preheated mould. Our results further show that when the impregnation time is a limiting factor, wet pressing appears to be a favourable approach for fast composite processing. Wet pressing was found to increase the available impregnation time by a factor of more than two due to the additional impregnation time gained as the resin and preform heat up when simultaneously placed in the tool. This approach has the additional advantage of lower direct tooling costs because of its simplicity, which is well suited for automated fast composite manufacturing.

We show that with the correct manufacturing process and processing conditions, the high exothermic reaction of the studied epoxy can be better controlled by determining appropriate processing parameters with our numerical models, thus avoiding inhomogeneous degree of cure respectively large variations in viscosity. These models will also allow to identify the benefit of novel fast curing resin formulation as proposed by the authors [4,5] and therefore representing a virtual processing test bench for novel fast curing matrix systems.

The models were solved as a two-dimensional section to gain a good understanding of how the different injection strategies influence the exothermic reaction, and hence the filling behaviour. Those models can be adapted to model more complex geometries and may be adapted to

describe other resin systems or CRTM methods, making them very powerful in numerically understanding compression RTM processing of next generation composite materials.

Acknowledgments

This research was supported by the Swiss Competence Center for Energy Research (SCCER) Efficient Technologies and Systems for Mobility, funded by the Commission for Technology and Innovation, SNF Project 200021_156011 and ETH Foundation grant SP-MaP 01–15. We also thank J. Maldonado and M. Grossman for the helpful discussions, and Huntsman Advanced Materials, Switzerland, for supplying materials.

References

- [1] Bader MG. Selection of composite materials and manufacturing routes for cost-effective performance. *Compos Appl Sci Manuf* 2002;33(7):913–34.
- [2] Baskaran M, de Mendibil I Ortiz, Sarrionandia M, Aurrekoetxea J, Acosta J, Argarate U, Chico D. Manufacturing cost comparison of RTM, HP-RTM and CRTM for an automotive roof in ECCM16. 2014. [Sevilla, Spain].
- [3] Simacek P, Advani SG, Iobst SA. Modeling flow in compression resin transfer molding for manufacturing of complex lightweight high-performance automotive parts. *J Compos Mater* 2008;42(23):2523–45.
- [4] Keller A, Masania K, Taylor AC, Dransfeld C. Fast-curing epoxy polymers with silica nanoparticles: properties and rheo-kinetic modelling. *J Mater Sci* 2016;51(1):236–51.
- [5] Keller A, Chong HM, Taylor AC, Dransfeld C, Masania K. Core-shell rubber nanoparticle reinforcement and processing of high toughness fast-curing epoxy composites. *Compos Sci Technol* 2017;147(Supplement C):78–88.
- [6] Maiarù M, D'Mello RJ, Waas AM. Characterization of intralaminar strengths of virtually cured polymer matrix composites. *Compos B Eng* 15 September 2018;149:285–95.
- [7] Liu B, Bickerton S, Advani SG. Modelling and simulation of resin transfer moulding (RTM)—gate control, venting and dry spot prediction. *Compos Appl Sci Manuf* 1996;27(2):135–41.
- [8] Laurenzi S, Grilli A, Pinna M, De Nicola F, Cattaneo G, Marchetti M. Process simulation for a large composite aeronautic beam by resin transfer molding. *Compos B Eng* 2014;57:47–55.
- [9] Palardy G, Hubert P, Ruiz E, Haider M, Lessard L. Numerical simulations for class A surface finish in resin transfer moulding process. *Compos B Eng* 2012;43(2):819–24.
- [10] Pham X-T, Trochu François, Gauvin Raymond. Simulation of compression resin transfer molding with displacement control. *J Reinforc Plast Compos* 1998;17(17):1525–56.
- [11] Gupta A, Kelly PA, Ehrgott M, Bickerton S. A surrogate model based evolutionary game-theoretic approach for optimizing non-isothermal compression RTM processes. *Compos Sci Technol* 2013;84:92–100.
- [12] Baskaran M, Aretxabaleta L, Mateos M, Aurrekoetxea J. Simulation and experimental validation of the effect of material and processing parameters on the injection stage of compression resin transfer molding. *Polym Compos* 2017<https://doi.org/10.1002/pc.24514>.
- [13] Mamoune A, Saouab A, Park C. Simple models of CRTM process. *Int J Material Form* 2008;1(1):911–4.
- [14] Sas HS, Erdal M. Modeling of particle–resin suspension impregnation in compression resin transfer molding of particle-filled, continuous fiber reinforced composites. *Heat Mass Tran* 2014;50(3):397–414.
- [15] Lefevre D, Comas-Cardona S, Binetruy C, Krawczak P. Coupling filtration and flow during liquid composite molding: experimental investigation and simulation. *Compos Sci Technol* 2009;69(13):2127–34.
- [16] Babeau A, Comas-Cardona S, Binetruy C, Orange G. Modeling of heat transfer and unsaturated flow in woven fiber reinforcements during direct injection-pultrusion process of thermoplastic composites. *Compos Appl Sci Manuf* 2015;77:310–8.
- [17] Nakouzi S, Pancrace J, Schmidt F, Le Maout Y, Berthet F. Simulations of an infrared composite curing process. *Adv Eng Mater* 2011;13(7):604–8.
- [18] Michaud V, Manson J-A. Impregnation of compressible fiber mats with a thermoplastic resin. Part I: theory. *J Compos Mater* 2001;35(13):1150–73.
- [19] Terzaghi K, Peck RB, Mesri G. *Soil mechanics in engineering practice*. John Wiley & Sons; 1996.
- [20] Multiphysics C. *COMSOL multiphysics reference manual*. COMSOL; 2013.
- [21] Olsson E, Kreiss G. A conservative level set method for two phase flow. *J Comput Phys* 2005;210(1):225–46.
- [22] Ruiz E, Trochu F. Thermomechanical properties during cure of glass-polyester RTM composites: elastic and viscoelastic modeling. *J Compos Mater* 2005;39(10):881–916.
- [23] Geissberger R, Maldonado J, Bahamonde N, Keller A, Dransfeld C, Masania K. Rheological modelling of thermoset composite processing. *Compos B Eng* 2017;124:182–9.
- [24] Bernet N, Michaud V, Bourban PE, Manson JAE. An impregnation model for the consolidation of thermoplastic composites made from commingled yarns. *J Compos Mater* 1999;33(8):751–72.
- [25] Wood JR, Bader MG. Void control for polymer-matrix composites (1): theoretical and experimental methods for determining the growth and collapse of gas bubbles. *Compos Manuf* 1994;5(3):139–47.
- [26] Neacsu V, Obaid AA, Advani S. Spontaneous radial capillary impregnation across a bank of aligned micro-cylinders—Part I: theory and model development. *Int J Multiphas Flow* 2006;32(6):661–76.
- [27] Studer J, Dransfeld C, Masania K. An analytical model for B-stage joining and co-curing of carbon fibre epoxy composites. *Compos Appl Sci Manuf* 2016;87:282–9.
- [28] Villière M, Lecoindre Damien, Sobotka Vincent, Boyard Nicolas, Delaunay Didier. Experimental determination and modeling of thermal conductivity tensor of carbon/epoxy composite. *Compos Appl Sci Manuf* 2013;46:60–8.